

Modelling Thermal Stratification and Artificial De-stratification using DYRESM; Case study: 15-Khordad Reservoir

Etemad - Shahidi, A. ^{1*}, Faghihi, M. ¹ and Imberger, J. ²

¹Enviro-Hydroinformatics COE School of Civil Eng., Iran University of Science and Technology, Tehran, Iran

²CWR, University of Western Australia, Nedlands, 6907, Australia

Received 25 Jan. 2009;

Revised 15 March 2010;

Accepted 25 March 2010

ABSTRACT: In this study, a one-dimensional model called DYRESM was used to simulate the thermal structure and artificial destratification of 15-Khordad Reservoir over a period of one year. The simulation showed that the reservoir is warm monomictic and is stratified during 210 days of the simulation year. The model reproduced the temperature of the meta- and hypolimnion very close to the observed data, but the temperature of the epilimnion was overestimated. As the meteorological data used for the simulation was collected in a nearby weather station, a sensitivity analysis was conducted to evaluate the effect of meteorological data bias on the simulation results. Air temperature, shortwave solar radiation, wind speed and vapour pressure were found to be, respectively, the most effective parameters. Furthermore, applications of two artificial destratification systems: bubble plume diffuser and surface mechanical mixer, were modelled. The sensitivity of the model outputs to the specifications of each system was investigated and the two systems were compared considering their efficiencies. It was revealed that the air diffusers were much more efficient than the mechanical mixers. This study showed that the DYRESM can accurately describe physical processes in this reservoir if the forcings are accurately given and the application of bubble is recommended for artificial destratification in this reservoir.

Key words: Modelling, De-stratification, Plume, Diffuser, Mixer, DYRESM, Simulation, Reservoir

INTRODUCTION

Thermal stratification is a natural phenomenon in lakes and reservoirs during summer. Solar radiation is absorbed by surface water and a well-mixed layer with low density and high temperature (epilimnion) is formed. The epilimnion is well mixed due to exposure to wind. The bottom layer (hypolimnion) remains dense and cold due to the extinction of solar radiation through the water column. Between these two layers, a strong thermal gradient zone (thermocline or metalimnion) inhibits vertical mixing. The thermocline acts as a barrier preventing active exchange of temperature, dissolved oxygen (DO), and dissolved nutrients between the reservoir surface and bottom layers (Sahoo & Luketina, 2006). Because of biological and biochemical oxygen consumption in the hypolimnion, dissolved oxygen decreases. As the replenishment of DO is restrained by the thermocline, the bottom layer faces anaerobic conditions. This condition in the hypolimnion leads to significant increase in the release of undesirable substances and deterioration of water quality.

In order to inhibit this deterioration, the rate of vertical transfer should be increased. Artificial destratification of the water column is a common mean for this purpose. Air bubbling, a continuous release of pumped air through diffusers in the bottom of lakes (Moshfeghi *et al.*, 2005), is the most popular artificial destratification method (Sahoo and Luketina, 2006). The rising bubbles entrain the ambient water. When the upwards buoyancy flux due to the air bubbles is equal to the downward force (due to the gravity) on the entrained water, the bubble plume sheds the entrained water. In this way, the heavy bottom water is lifted up and mixed with the lighter water in the top layer. The bubble plume then begins to entrain the ambient water again, until it reaches the surface where any entrained water is shed. Continuation of this process mixes the water column thoroughly.

The application of surface mechanical mixer is another artificial destratification system. This system consists of a large impeller mounted at the surface of the water body which points vertically downwards.

*Corresponding author E-mail: etemad@iust.ac.ir

The impeller is surrounded by a non-permeable curtain (a draft tube), through which water is impelled until escaping at the end of the draft tube. Once reaching the end of the draft tube, the water rises, enters the ambient water and mixes the water column.

The aim of this study is to simulate the performance of different destratification systems in the 15-Khordad reservoir using DYRESM. The DYRESM (DYnamic REservoir Simulation Model) (Schladow and Hamilton, 1997) is a calibration-free, process-based, one-dimensional hydrodynamic model for the simulation of vertical distribution of temperature, salinity and density in lakes and reservoirs. This model is also capable of simulating artificial destratification systems.

15-Khordad Reservoir is located at 34°102 N and 50°302 E, in Qom, Iran. The dam is constructed on the brackish river, Qomrood, to supply the drinking water for Qom. The capacity of the reservoir is 200 MCM and it is designed to provide an average supply of 37.4 MCM per year for drinking and 28.3 MCM per year for agriculture purposes. The surface area of the reservoir is 13.5 km² and the length is 12 km. The average flow rate of the river is 5.61 m³/s varying from 1 m³/s in summer to 14.5 m³/s in spring. The average salinity of the inflowing river is 1525 mg/L varying from 1235 to 2219 mg/L, entering 266000 tons of salt into the reservoir each year. Considering the high salinity of the inflowing river and the dominant stratification, the study of the influence of the stratification and destratification on the dynamics of this water body is vital.

MATERIALS & METHODS

15-Khordad Reservoir is located at 34°102 N and 50°302 E, in Qom, Iran. The dam is constructed on the brackish river, Qomrood, to supply the drinking water for Qom. The capacity of the reservoir is 200 MCM and it is designed to provide an average supply of 37.4 MCM per year for drinking and 28.3 MCM per year for agriculture purposes. The surface area of the reservoir is 13.5 km² and the length is 12 km. The average flow rate of the river is 5.61 m³/s varying from 1 m³/s in summer to 14.5 m³/s in spring. The average salinity of the inflowing river is 1525 mg/L varying from 1235 to 2219 mg/L, entering 266000 tons of salt into the reservoir each year. Considering the high salinity of the inflowing river and the dominant stratification, the study of the influence of the stratification and destratification on the dynamics of this water body is vital. The DYRESM was developed in the Water Research Centre of the University of Western Australia. An extensive description of the model has been given in the Imberger and Patterson (1981), Hocking et al. (1988) and Hocking and Patterson (1991) studies. In

brief, it is a one-dimensional model, which simulates the vertical distribution of temperature and salinity in lakes and reservoirs. The model assumes horizontal homogeneity, which is based on the density stratification usually found in reservoirs. Density stratification inhibits the vertical motions while the horizontal variations in density are quickly relaxed by the horizontal advection and convection.

The one dimensional assumption is valid when $L_N \gg 1$, $L_{NI} \gg 1$, $F_O \ll 1$ and $R \gg 1$; where L_N is the ratio between restoring force and distributing force introduced by the wind (Imberger and Paterson, 1990), L_{NI} is the ratio between restoring force and distributing force introduced by plunging inflow, F_O is the ratio between outflow distributing force and restoring force and R is the ratio between Rossby radius of deformation and lake dimensions.

The physics of the DYRESM is based on the following processes: (1) surface heat and mass transfer; (2) energetics of the surface layer; (3) vertical diffusion in the hypolimnion; (4) inflow and outflow dynamics; (5) air bubble plume dynamics; and (6) water plume dynamics. The model is based on the Lagrangian layer scheme (i.e., the layers are adjusted to stay within user-defined limits; a fixed grid approach would be an Eulerian scheme), in which the lake is modelled by a series of horizontal layers of uniform property but variable thickness. These layers can expand, contract, amalgamate, divide and move up and down as they are affected by the inflow, outflow, evaporation and rainfall or according to the physical processes represented in the model.

The main advantage of the DYRESM, compared to the other models, is its ability to simulate destratification systems. In modelling the air bubbler destratification, the model uses the simple buoyant plume equations, and assumes the plumes are circular and non-interacting. The bubbler is initialized by first computing the upwards buoyancy flux due to the air (Fischer *et al.*, 1979):

$$B_{air} = gQ_{diff} \quad (1)$$

Q_{diff} is the air flow rate of the diffuser at its level.

Once the value of Q_{diff} is passed into the model, it is divided by the number of ports (or clusters) to determine the flow rate per port. All the subsequent calculations are done on a per port basis, and then outcomes are multiplied by the total number of ports to get the total effect of the destratification system. The flow rate of entrained water is computed as (Fischer *et al.* 1979):

$$Q_p = \alpha \frac{6\pi}{5} b_1 L_R B^{1/3} z^{5/3} \quad (2)$$

where B is the buoyancy flux [m^4/s^3], z is the bottom layer thickness [m], b_1 is a constant (4.7 according to Fischer *et al.*, 1979), L_R is the plume aspect ratio (plume radius to plume length, assumed to be a constant of 0.1) and α is an entrainment coefficient. As the bubbles rise upward, they expand adiabatically due to the decrease of the pressure. The new flow rate of bubbles is calculated according to Wallace and Hobbs (1977):

$$Q_i = Q_{i-1} \left(\frac{P_{i-1}}{P_i} \right)^{0.71} \quad (3)$$

where P is the pressure and $i-1$ refers to the layer below. The combined buoyancy flux of the air bubbles and entrained water is calculated as:

$$B_i = gQ_i - g \left(\frac{\rho_i - \rho_p}{\rho_i} \right) Q_p \quad (4)$$

where ρ_i is the density of the current layer, and Q_p is the flow rate of the entrained volume. The second term is the reduction in buoyancy flux due to the entrained water which the plume is dragging. The flow rate of the entrained volume in the layer i is calculated as :

$$Q_p = \alpha \frac{6\pi}{5} b_1 L_R B^{1/3} z_i^{5/3} - z_{i-1}^{5/3} + Q_{p,i} \quad (5)$$

When the combined buoyancy flux becomes zero or negative, the entrained water detrains from the air plume. It is then routed to its neutrally buoyant level instantaneously. The plume characteristics are then reset, and the air continues to rise and begins entraining the water again.

In modelling the surface mechanical mixers, the model assumes that water acts as a buoyant plume when exiting from the draft tube. The plume is modelled as a line plume, wrapped around the circumference of the circular draft tube. The plume is initialized by computing the upwards buoyancy flux due to the difference in density between the water in the draft tube (assumed to have the same properties as the surface layer water) and the water at the base of the draft tube (Fischer *et al.*, 1979):

$$B = g \frac{\rho_{base} - \rho_{plume}}{\rho_{base}} \frac{Q_p}{\pi D} \quad (6)$$

where Q_p is the daily average impeller flow rate (m^3s^{-1}), and D is the draft tube diameter in meter. The unit of B is (m^3s^{-3}), which describes the buoyancy flux per unit length for a line plume (Fischer *et al.*, 1979). The new flow rate due to the entrained water is computed as (Fischer *et al.*, 1979):

$$Q_p = 3.32\alpha(\pi D)B^{1/3}\Delta z_j + Q_p \quad (7)$$

where Δz_j is the starting layer thickness (the layer thickness at the base of the draft tube), and α is an entrainment coefficient, found experimentally to be 0.1024 (Fischer *et al.*, 1979). This number has been halved for this application, as the ambient water is only being entrained along one side of the plume due to the vertical barrier of the draft tube. When the plume reaches the neutral buoyancy, the buoyancy flux becomes zero and the plume is instantaneously inserted. As the plume is single phase, there is no re-initialization after detrainment, as occurs for the bubble plumes. The simulations were conducted over a 12-month period between April 1997 and April 1998. Daily averaged inflow volume and temperature and outflow volume were available in the simulation period, but the inflow salinity was only measured once or twice in a month in normal conditions, and the results were considered as monthly average. All the required meteorological data were obtained from a nearby weather station located at 34°422 N and 50°512 E. The monthly measured temperature and salinity profiles in the deepest part of the reservoir were used for model calibration. The light extinction coefficient, was not measured so its value was calibrated to obtain the best fit between measured and simulated temperatures.

As difference existed between observed and simulated surface water temperatures, a sensitivity analysis was conducted to reveal the most important parameters affecting the epilimnion temperature. Short and long wave radiation, air temperature, wind speed, vapour pressure, inflow temperature and light extinction coefficient were selected as the parameters to be investigated. Finally, in order to evaluate the application of a destratifying system to the reservoir, firstly, two destratification systems were modelled and compared to each other. The characteristics of each system which affect its efficiency were also evaluated.

RESULTS & DISCUSSION

The simulation results showed that the reservoir was stratified approximately 210 days in the simulation year, and was warm monomictic because it was mixed once in a year, and the water temperature did not drop below 4°C (Fig. 1). The Comparison of the simulated surface elevation with the measured one showed that the conservation of mass is correct in the model as the computed absolute mean error was 1.30%.

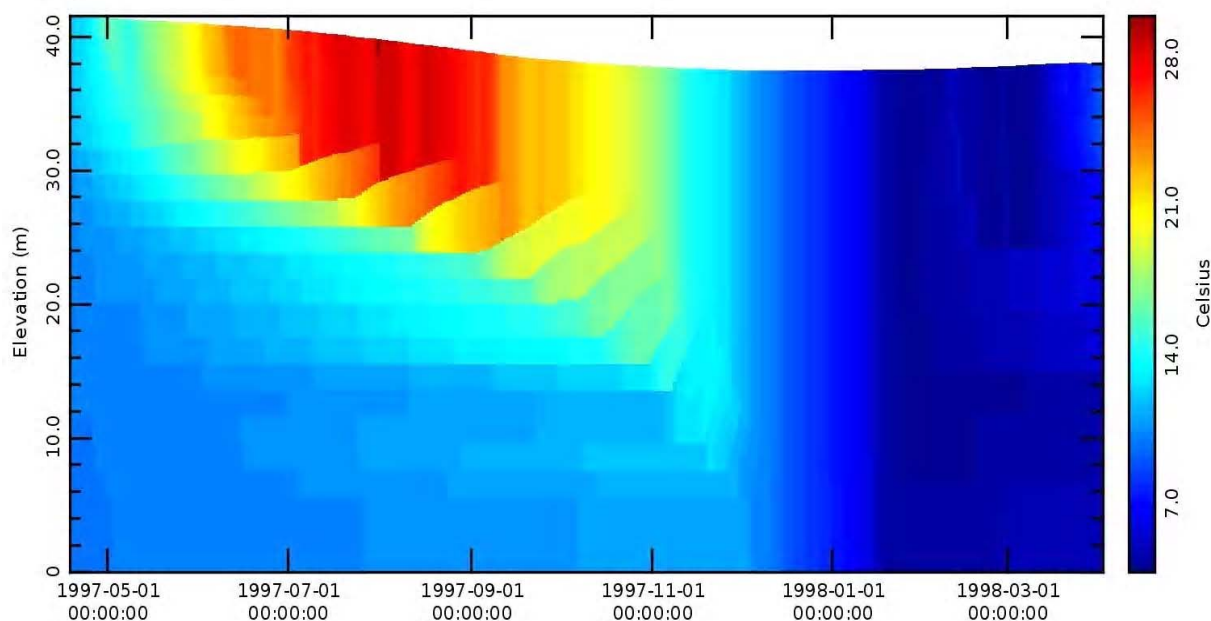


Fig. 1. Thermal stratification of the 15khordad Reservoir

DYRESM assumes that the light extinction coefficient of water remains constant during the simulation period. While changing this coefficient for the model calibration, it was revealed that higher values of the light extinction coefficient cause the surface layer to become warmer, the hypolimnion to become cooler and the thermocline to rise up nearer to the surface. Reducing this coefficient had the opposite effect. In the 15-Khordad Reservoir the best fit of the simulation results to the field measurements was obtained with the light extinction coefficient of 0.15 m^{-1} . Using this value, the absolute mean error of the simulation was 5% (0.66 to 6.94%). As shown in Fig. 2. in the stratified period, the hypolimnion and metalimnion temperatures were simulated close to the measured profiles, but the epilimnion temperature was overestimated. The observed error could be caused by the inaccuracy in input data. The existing difference between the real values of meteorological data in the reservoir and the measured values in the nearby station is the most important point. In order to define the most affective parameters on the epilimnion temperature, a sensitivity analysis was conducted as follows:

Long wave radiation: This parameter is given to the model as the fraction of sky covered with clouds. The DYRESM calculates the net long wave radiation considering the reflection from the clouds. Higher cloud cover causes more long wave radiation emitted to the reservoir. Long wave radiation is mostly absorbed or emitted from the surface layer, so it directly affects the

surface layer and makes it warm. However, in the study area, the sky is almost clear through out the year. The mean coverage of the sky (clouds) during the simulation period is only 2%. Hence, the long wave radiation is always at its lowest level, and the high surface temperature cannot be due to the overestimation of this parameter.

Short wave radiation: The wavelengths between 280 nm and 2800 nm were measured directly. The model divides the short wave radiation into penetrative and non-penetrative. Radiation shorter than 700 nm (Photosynthetically Active Radiation, or PAR) is considered to be penetrative and is distributed through the water column. This has been found experimentally to be approximately 45% of incoming solar radiation (Gates, 1966; Jellison and Melack, 1993). The DYRESM therefore assumes that 55% of the incoming solar radiation is non-penetrative and it is absorbed or emitted from the surface layer.

In order to evaluate the effect of uncertainty in this parameter on the simulation results, 20% increase and 20% decrease in the incoming short wave radiation were adopted. Results showed that in the stratified period, 20% increase in short wave radiation causes 6% (1°C) increase in the surface layer temperature and 2% (0.3°C) increase in the bottom layer temperature. When the reservoir is mixed, this increase caused 20% (1.10°C) increase in the water column temperature. With 20% decrease, the results were exactly opposite. Hence, the accuracy in measuring short

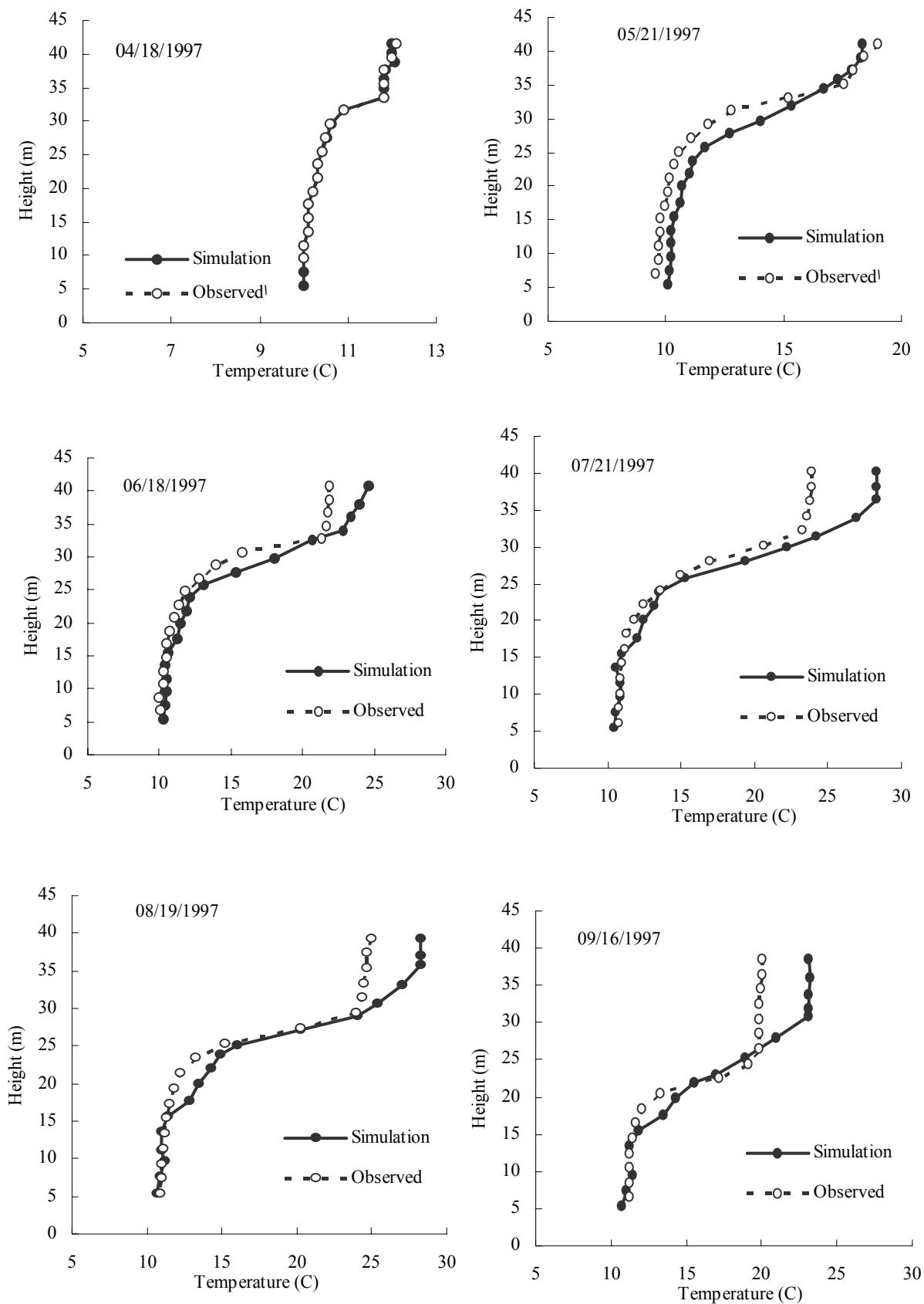


Fig. 2. Comparison between observed and simulated temperatures on different dates (Continues)

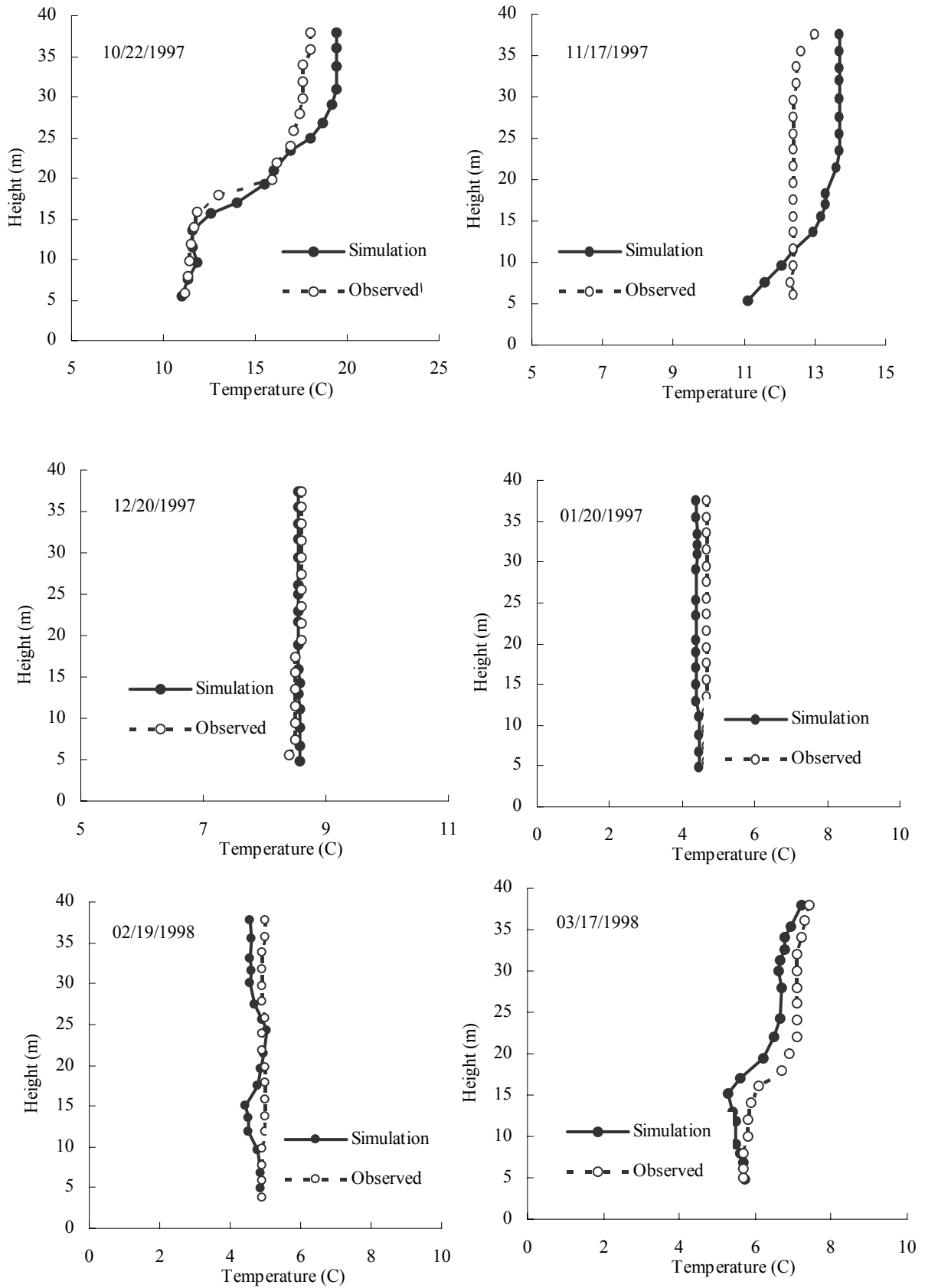


Fig. 2. Comparison between observed and simulated temperatures on different dates (Coutinuation)

wave radiation has a considerable effect on the simulation results.

Vapour pressure: Using the measured values of dry bulb air temperature and relative humidity of the air, this parameter was calculated using equation C2 of TVA (1972). Vapour pressure affects evaporation from the surface layer, and as the evaporation is a mechanism through which water loses energy, the vapour pressure affects the surface layer temperature. For evaluation of this effect, a simulation was conducted considering $\pm 20\%$ change to this parameter. Results showed that 20% increase in the vapour pressure, in the stratified period, caused the epilimnion temperature to increase 1.40% (0.35°C), but the hypolimnion remained unchanged. In the mixed period, this increased the water column temperature by approximately 10% (0.50°C). For 20% decrease in the vapour pressure, the results were vice versa.

Wind speed: Similar to the vapour pressure, by altering evaporation from the surface layer, wind speed affects the epilimnion temperature. Simulations' results indicated that, in the stratified period, 25% increase in the wind speed caused 5% (1.20°C) decrease in the epilimnion temperature while the hypolimnion temperature remained unchanged. In the mixed period, this increase caused 10% decrease in the water column temperature. Reducing the wind speed by 25% increased the epilimnion temperature by 1.10% (0.3°C) and did not affect the hypolimnion. In the mixed period, the water column temperature increased 13% (0.65°C) due

to 25% decrease in the wind speed.

Thus, increasing the wind speed increases the evaporation from the surface layer and decreases its temperature. Vice versa, increasing the wind speed decreases the epilimnion temperature. In addition, it could be concluded that increasing the wind velocity had a stronger impact on the epilimnion temperature than decreasing it.

Air temperature: Thermal interactions between water and air are considerable. Air temperature varies significantly in different areas, so the difference between real values in the reservoir location and the measured values in the station might be considerable. The simulation showed that increase in air temperature significantly increases the epilimnion temperature without changing the hypolimnion temperature, and vice versa decreasing the air temperature decreases the surface water temperature. Under the case of 20% decrease in the air temperature, the simulated results matched the measured profiles very well. As the $\pm 20\%$ change in the air temperature caused $\pm 12.3\%$ change in the surface water temperature, the air temperature was recognized as the most affecting parameter. In Table 1. the outcomes of this analysis are given briefly.

As the air temperature and short wave radiation were found to be the most important parameters affecting the surface water temperature, the effect of applying daily averages values of these parameters was evaluated by running the model with hourly val-

Table 1. Sensitivity analysis of different parameters affecting the reservoir temperature

Altered variable	Change	Stratified period		Mixed period
		Epilimnion	Hypolimnion	Water column
Air temperature	+20%	+12.3%	0	+7%
	-20%	-12.3%	0	-9%
Short wave radiation	$\pm 20\%$	$\pm 6\%$	$\pm 2\%$	$\pm 20\%$
Wind speed	+25%	-5%	0	-10%
	-25%	+1.10%	0	+13%
Vapour pressure	$\pm 20\%$	$\pm 1.40\%$	0	$\pm 10\%$
Inflow temperature	$\pm 20\%$	Negligible	Negligible	Negligible

ues. The model was run for one month with hourly values of these two parameters while the other parameters were set to be constant through out each day. Simulation results showed that the only parameter which varied in different hours of a day was the surface layer temperature, and this variation was about 0.77°C. The lowest surface water temperature occurred at 9:00 and the highest one at 18:00 (Fig. 3). Consequently, the application of daily average of parameters did not significantly decrease the model's accuracy.

Bubble plume destratification: In the DYRESM, the characteristics of bubble diffusers are the number of diffusers, height of diffuser above the lake bottom, number of ports of the diffuser, air flow rate of diffuser and the type and length of operation. Three types of operation for artificial destratification can be modelled in the DYRESM: daytime operation, night-time operation and continuous operation. First, one diffuser with 100 ports and air flow rate of 0.1 m³/s, which was located 4 meters above the reservoir bottom and operated continuously during the reservoir stratification (200 days), was modelled. Results of simulation showed that after approximately 3 weeks of operation, the reservoir destratified (Fig. 4). In addition, increasing the air flow rate of diffuser increased the rate of destratification (Fig. 5) and decreasing the number of ports had the same effect. It is due to the fact that the reduction of the number of ports increases the air flow rate from each port. Slip velocity and the size of bubbles increase when the air flow rate increases. It should be mentioned that the rate of destratification is a function of these two parameters and increases with their increase.

in Fig. 6. a diffuser located 4 meter above the bottom destratifies the reservoir, but locating a diffuser 10 meter above the bottom just deepens the thermocline and the stratification remains unchanged. Hence, the diffuser should be located as near as possible to the bottom of reservoir, and the only consideration needed is the avoidance of sediment resuspension.plume interaction. In order to evaluate the effect of the number of diffusers on the destratification rate, two diffusers with air flow rate of 0.1 m³/s were modelled. As seen in Fig. 7. compared to Figs. 4 and 5, results indicated that the operation of two diffusers simultaneously was more effective on destratification rate. Consequently, the most effective parameters on bubbler destratification rate were number of diffusers, air flow rate, number of ports and diffuser height, respectively.

Surface mechanical mixer: As the difference between the surface and bottom water densities, compared to the difference between density of water and air, is very low and the formed plume in this case is single phase; it is predicted that the efficiency of the surface mechanical mixers in destratifying the reservoir will be less than that of bubble diffusers.Characteristics of this destratifying system are: the length and diameter of draft tube, flow rate of water, number of destratification devices, and type and length of operation. A continuous operating surface mechanical mixer during the stratified period of the reservoir (200 days) with flow rate of 1 m³/s was modelled. The diameter of the draft tube and its lengths were selected 2 and 35 meters, respectively. Fig. 8 shows the performance of this mixer in destratifying the res-

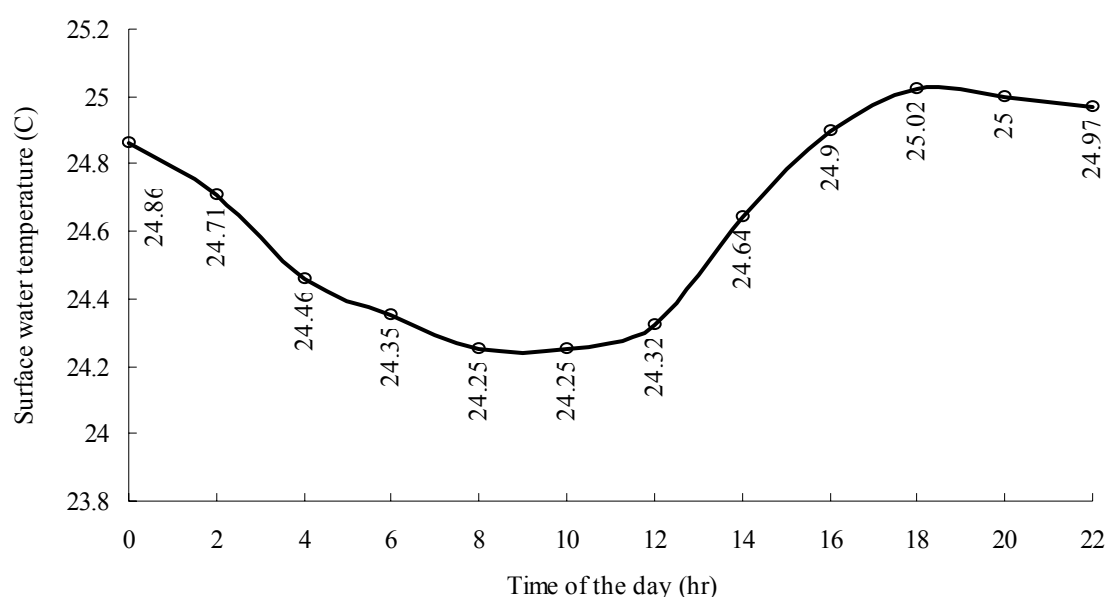


Fig. 3. variation of surface water temperature in different hours of a day

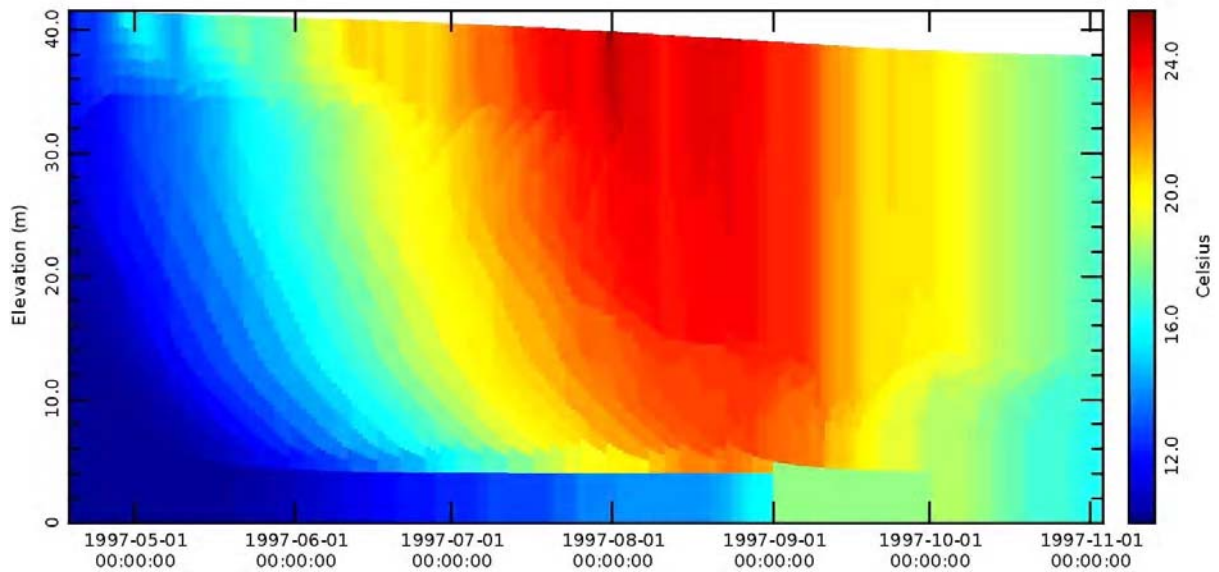


Fig. 4. Destratification of the reservoir with bubble diffuser ($Q = 0.1 \text{ m}^3/\text{s}$, 100 ports, 4 meter above the bottom)

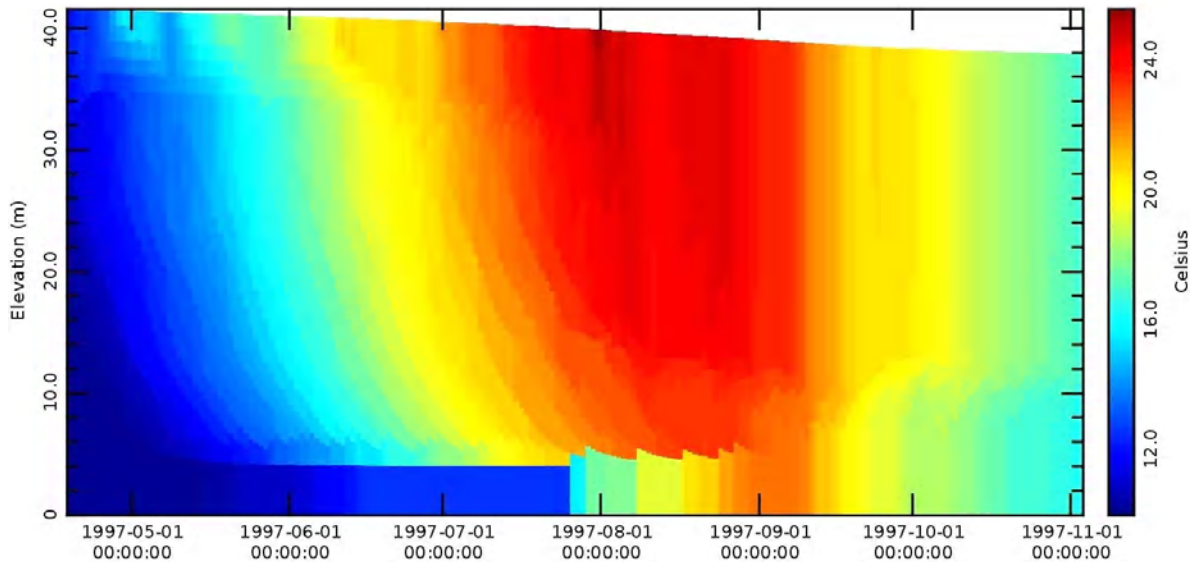


Fig. 5. Destratification of the reservoir with bubble diffuser ($Q = 0.3 \text{ m}^3/\text{s}$, 100 ports, 4 meter above the bottom)

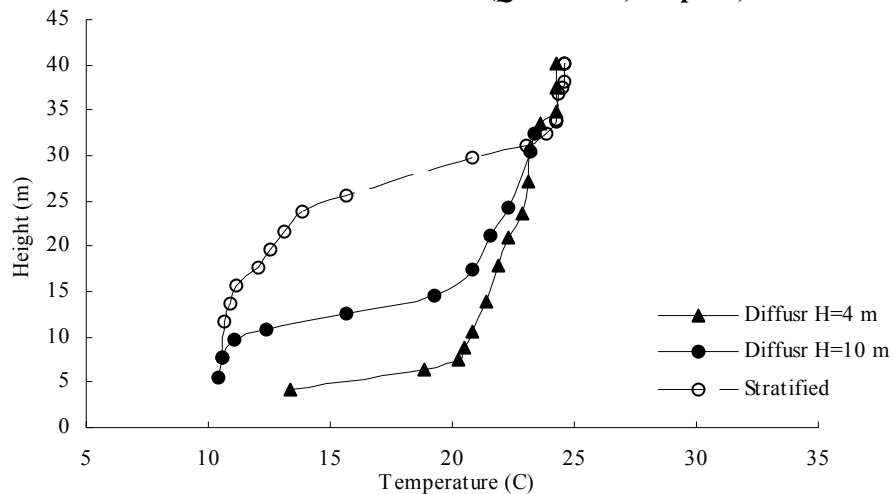


Fig. 6. Comparing the thermal profile of the reservoir in three cases: (1) stratified reservoir, (2) destratified with a diffuser located 10 meter above the bottom, and (3) destratified with a diffuser located 4 meter above the bottom

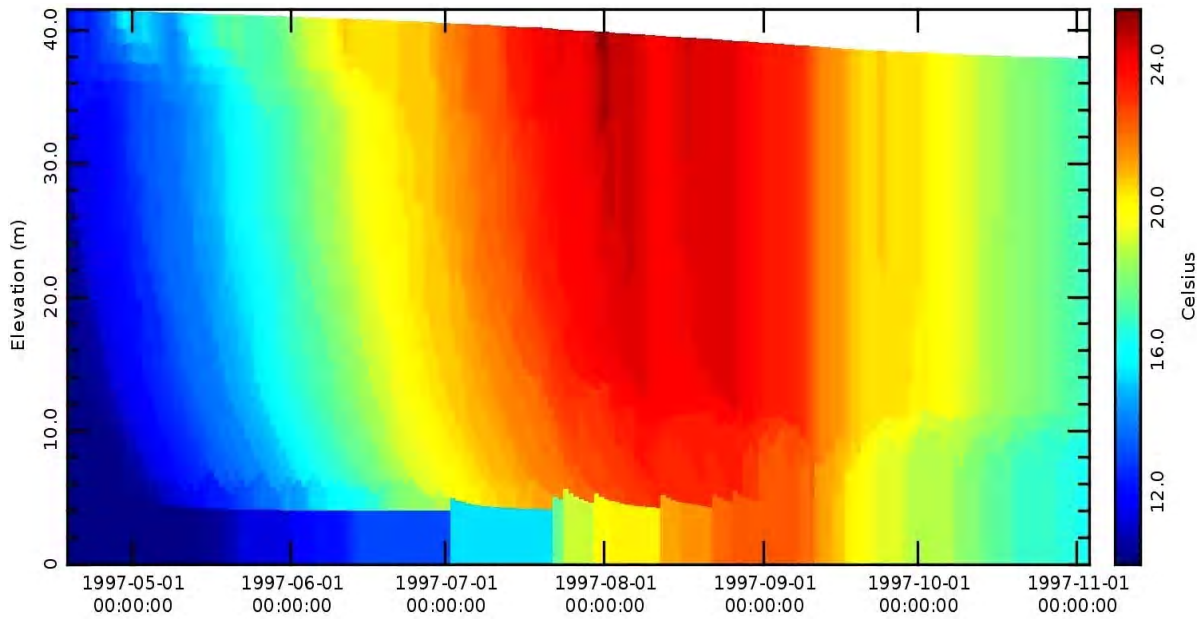


Fig. 7. Destratification of the reservoir with two bubble diffuser ($Q = 0.1 \text{ m}^3/\text{s}$, 100 ports, 4 meter above the bottom)

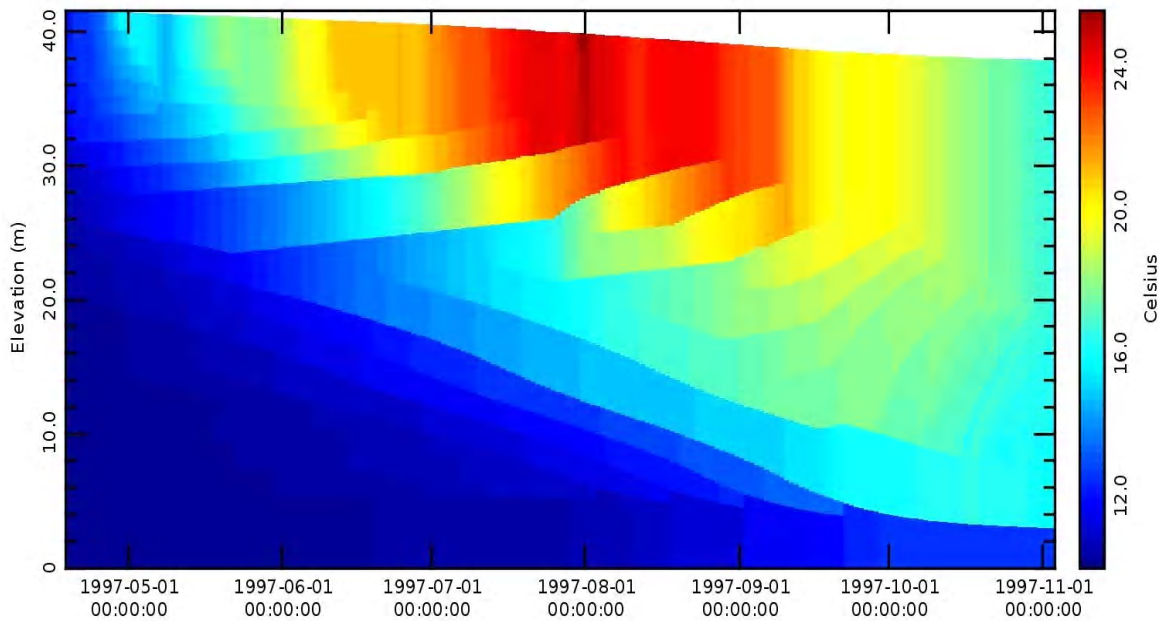


Fig. 8. Destratification of the reservoir with one mixer ($Q = 1 \text{ m}^3/\text{s}$, draft tube: $L=35\text{m}$, $D=2\text{m}$)

ervoir. As seen, this mixer is not capable of destratifying the reservoir although the water flow rate of $1 \text{ m}^3/\text{s}$ is very high. The effect of increasing the flow rate to $3 \text{ m}^3/\text{s}$ is shown in Fig. 9. Increasing the diameter of draft tube is also effective in increasing the destratification rate. Fig. 10 shows the results of simulated mechanical mixer with 1 meter increase in draft tube diameter. Considering the equations 6 and 7 and comparing Fig. 10 with Fig. 9, it can be concluded that the diameter of draft tube was more effective in destratification rate than the water flow rate. Same as diffusers, the number of destratifying devices was the

most effective parameter in mixers, and the length of draft tube, like the diffuser height, only affected the thermocline depth and is not important in destratification rate. In order to gain a destratification rate close to that of a diffuser, the number of mixers, diameter of draft tube and water flow rate were increased. The result is shown in Fig. 11. As observed, the efficiency of three mixers with flow rate of $3 \text{ m}^3/\text{s}$ and diameter of 5 meter was approximately close to that of a diffuser with air flow rate of $0.1 \text{ m}^3/\text{s}$ and 100 ports (Fig. 4). Consequently, the bubble diffuser efficiency in destratification compared with mechanical

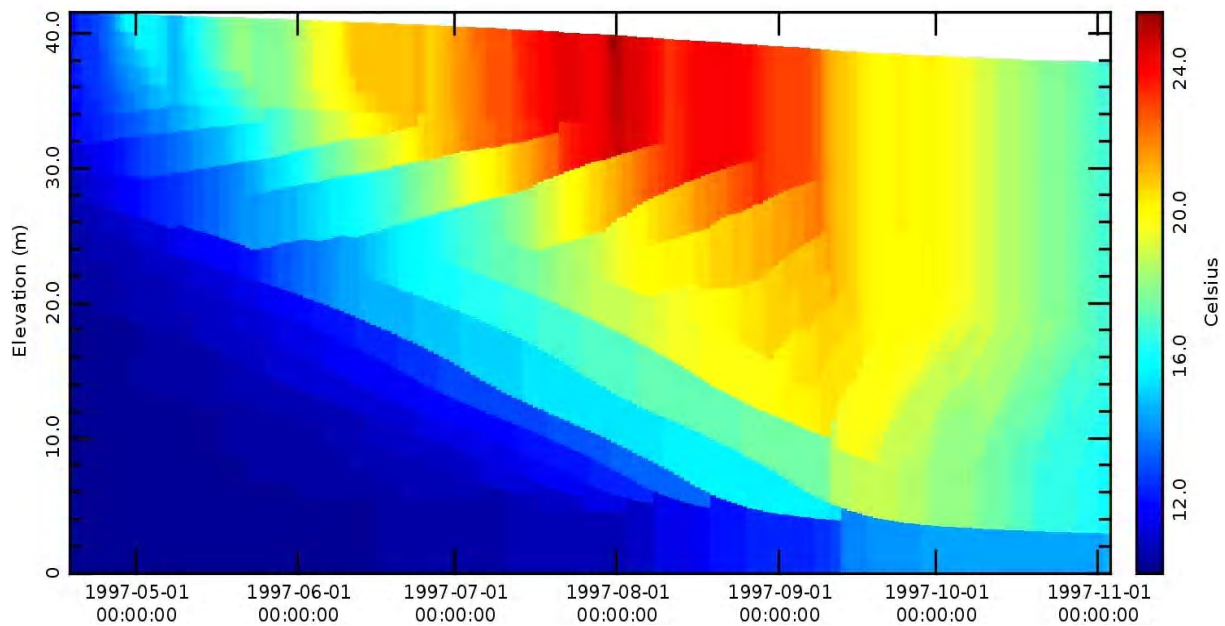


Fig. 9. Destratification of the reservoir with one mixer ($Q = 3 \text{ m}^3/\text{s}$, draft tube: $L=35\text{m}$, $D=2\text{m}$)

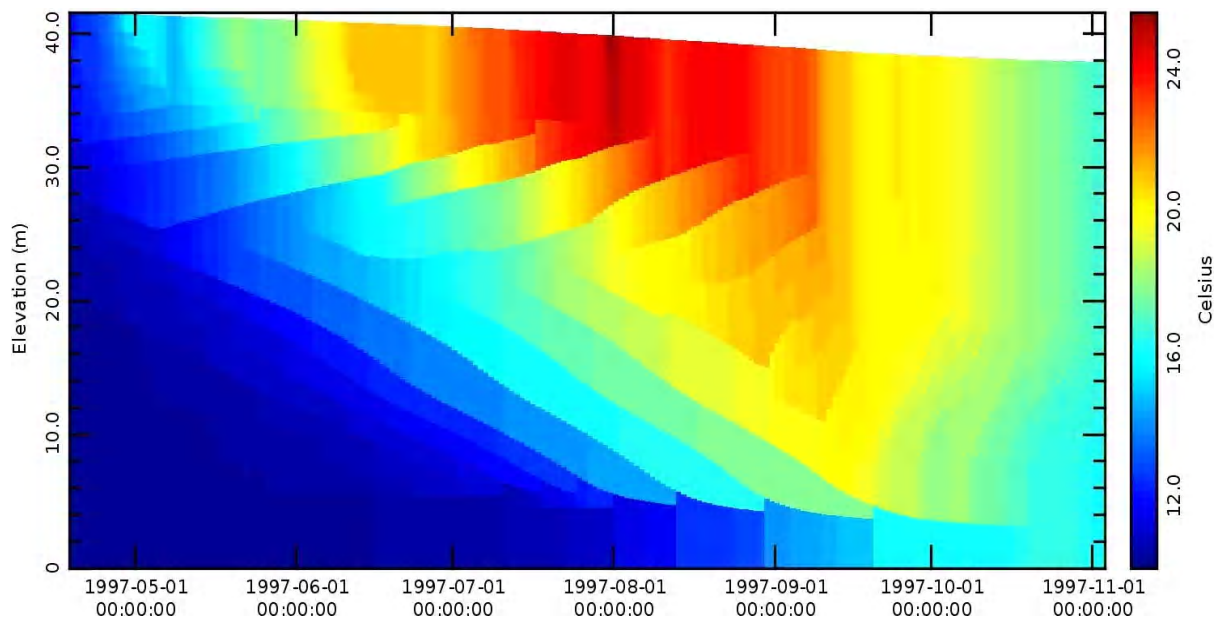


Fig. 10. Destratification of the reservoir with one mixer ($Q = 3 \text{ m}^3/\text{s}$, draft tube: $L=35\text{m}$, $D=3\text{m}$)

mixers is very high and the use of mechanical mixers is not recommended.

CONCLUSION

This study showed that the DYRESM can accurately describe physical processes in reservoirs if the input data are accurately given. In the 15-Khordad Reservoir the air temperature, short wave radiation, wind speed and vapour pressure mainly control the thermal structure. Therefore, it is strongly recommended that these parameters, specifically air temperature and short wave radiation, to be measured in situ. Also, accurate measurements of light extinction coefficient are recom-

mended to be carried out because this coefficient affects the thermocline position. Modelling the destratification devices shows that in diffusers, the number of diffusers, air flow rate and number of ports; and in mechanical mixers, the number of mixers, diameter of the draft tube and water flow rate, are respectively important in the destratification rate. Height of the diffuser above the bottom of the lake and the length of the draft tube only control the thermocline depth and do not affect the destratification rate. Considering these devices efficiencies, application of bubble diffusers rather than mechanical mixers is recommended for artificial destratification in this reservoir.

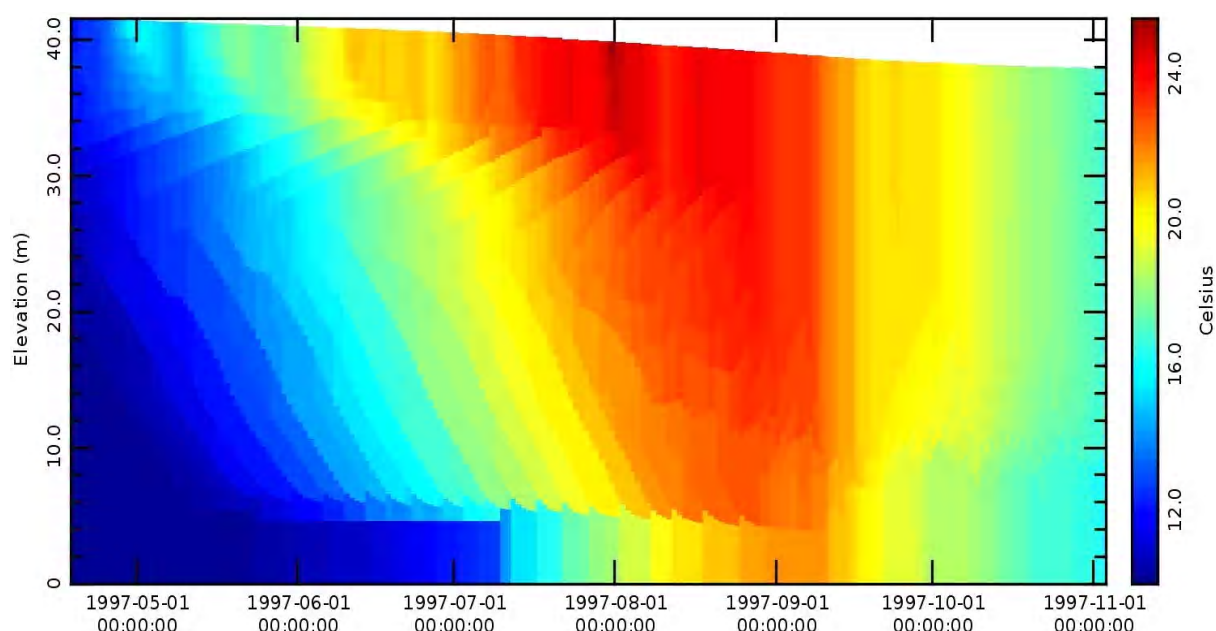


Fig. 11. Destratification of the reservoir with three mixer ($Q = 3 \text{ m}^3/\text{s}$, draft tube: $L=35\text{m}$, $D=5\text{m}$)

ACKNOWLEDGEMENTS

This work was partly supported by the deputy of research, Iran University of Science and Technology. The first author would like to acknowledge CWR, University of Western Australia for receiving the Gladden senior visitor fellowship. The authors also have their special appreciation to Dr. Matthew Hipsey, whose helps led to substantial improvement of this study.

REFERENCES

CWR (2005). DYRESM - Scientific Reference Manual. Centre for Water Research, University of Western Australia.

Fischer, H.B., List, E.G., Koh, R.C.Y., Imberger, J., and Brooks, N.H., 1979. Mixing in inland and coastal waters. Academic Press.

Gal, G., Imberger, J., Zohary, T., Antenucci, J., Anis, A. and Rosenberg, T. (2003). Simulating the thermal dynamics of Lake Kinneret. *Ecol. Model.*, **162**, 69-86.

Gates, D.M. (1966). Spectral distribution of solar radiation on the earth's surface. *Science*, **151**, 523-529.

Hamilton, D.P. and Schladow, S.G. (1997). Prediction of water quality in lakes and reservoirs. Part I - Model description. *Ecol. Model.*, **96**, 91-110.

Han, B.P., Armengol, J., Garcia, J. C., Comerma, M., Roura, M., Dolz, J. and Straskraba, M. (2000). The thermal structure of Sau Reservoir (NE: Spain): a simulation approach. *Ecol. Model.*, **125**, 109-122.

Henderson-Sellers, B. (1986). Calculating the surface energy balance for lakes and reservoir modelling: a review. *Rev. Geograph.*, **24**, 625-649.

Hocking, G.C., Sherman, B.S. and Patterson, J. C. (1988). Algorithm for selective withdrawal from stratified reservoirs. *J. Hydr. Engng., ASCE.*, **114(7)**, 707-719.

Hocking, G.C. and Patterson, J. C. (1991). A quasi two-dimensional reservoir simulation model. *J. Environ. Eng. Div., ASCE.*, **117**, 595-613.

Imberger, J. and Patterson, J.C. (1981). A dynamic reservoir simulation model - DYRESM: 5. (In: Fischer, H.B. (ed.), *Transport Models for Inland and Coastal Waters*. Academic Press.

Imberger, J. and Patterson, J.C. (1990). Physical limnology. *Adv. in Appl. Mech.* **27**, 303-455.

Jellison, R. and Melack, J.M. (1993). Meromixis in hypersaline Mono lake, California. stratification and vertical mixing during the onset, persistence and breakdown of meromixis. *Limnol. Oceanogr.*, **38**, 1008-1019.

Moshfeghi, H., Etemad-Shahidi, A. and Imberger, J. (2005). Modelling of bubble plume destratification using DYRESM. *J. Wat. Sup. Res. & Tech.-AQUA.*, **54**, 37-46.

Sahoo, G.B. and Looketina, D. (2006). Response of a tropical reservoir to bubbler destratification. *J. Env. Eng.*, **132(7)**, 736-746.

Schladow, S.G. and Fischer, I.H. (1995). The physical response of temperate lakes to artificial destratification. *Limnol. Oceanogr.*, **40(2)**, 359-373.

Schladow, S.G. and Hamilton, D.P. (1997). Prediction of water quality in lakes and reservoirs. Part II - Model calibration, sensitivity analysis, verification and validation. *Ecol. Model.*, **96**, 111-123.

Tennessee Valley Authority, (1972). Heat and mass transfer between a water surface and atmosphere. *Water Resources Research Laboratory Report 14*, Report No. 0-6803.

Wallace, J.M. and Hobbs, P.V. (1977). *Atmospheric Science: an introductory survey*. Academic Press.